NUCLEAR REACTIONS -- THEORY

TRANSVERSE MOMENTUM DISTRIBUTIONS IN INTERMEDIATE ENERGY HEAVY-ION COLLISIONS

G.F. Bertsch, W.G. Lynch and M.B. Tsang

We examine the sensitivity of nucleon transverse momentum distributions to nucleon-nucleon collisions and to the nuclear equation of state using the Boltzmann equation which includes the mean field term and the collision integral. The Boltzmann equation, given below, describes the time evolution of the Wigner-function $f(\vec{r},\vec{k},t)$ in phase space.[1]

$$\frac{\partial f}{\partial t}_1 + \vec{v}\cdot\vec{\nabla}_r f_1 - \vec{\nabla}_r U\cdot\vec{\nabla}_p f_1 =$$

$$\frac{4}{(2\pi)^3}\int d^3k_2 d^3k_3 d\Omega \;\; \sigma_{nn}(\Omega)\; v_{12}[f_3 f_4(1-f_1)(1-f_2)$$

$$-f_1 f_2(1-f_3)(1-f_4)]\delta^3(\vec{k}_1+\vec{k}_2-\vec{k}_3-\vec{k}_4) \qquad (1)$$

Here, $\sigma_{nn}(\Omega)$ and v_{12} are the cross section and relative velocity for the colliding nucleons, and U is the mean field potential approximated by

$$U = - a_1\rho/\rho_o + a_2(\rho/\rho_o)^\gamma \qquad (2)$$

For simplicity, $\sigma_{nn}(\Omega)$ was taken to be constant and isotropic. Details concerning the solution of this equation are contained in Ref. 1.

Calculations were performed with the mean field potentials and nucleon-nucleon cross sections given in table 1. Collisions between mass 40 projectiles and mass 40, 100, and 197 targets were calculated for bombarding energies of E/A = 60, 100, 200, and 400 MeV and impact parameters of 3, 5, 7, and 9 fm. Here we report results concerning the momentum distributions of emitted nucleons. The nucleon mean transverse momentum, $\langle P_x\rangle$, was calculated by averaging over the distribution of nucleon momenta in the reaction plane perpendicular to the beam

Table 1

set	mean field	a_1(MeV)	a_2(MeV)	K(MeV)	γ	$4\pi\sigma_{nn}(\Omega)$(mb)
1	soft	356	303	200	7/6	41
2	stiff	124	70.5	375	2	41
3	soft	356	303	200	7/6	20
4	stiff	124	70.5	375	2	20

Table 1: Nuclear mean field parameters and nucleon-nucleon cross sections used in the calculations.

momentum. To facilitate discussion, we designate the z-axis to be parallel to the projectile linear momentum; the x-axis is chosen to lie in the reaction plane. For non-zero impact parameters, the projectile is displaced to positive values of x; positive $\langle P_x\rangle$ (negative $\langle P_x\rangle$) corresponds to emission to the same (opposite) side of the target as the initial impact. To avoid cancellations between the transverse momenta of nucleons emitted parallel and antiparallel to the projectile momentum, nucleons emitted at center-of-mass angles greater than 90° were excluded in the determination of $\langle P_x\rangle$. We examined the phase Qbdua distribution of nucleons at time intervals of 50 fm/c, 100 fm/c and 200 fm/c from the start of the collision and chose a time interval long enough for the final state residues to be well separated. Evaporation from the target-like residue was suppressed by excluding nucleons located within a sphere of radius $R=1.4A_{tgt}^{1/3}$ about the target-like residue and by excluding nucleons with laboratory energies less than 15 MeV. The results are relatively insensitive to details concerning the exclusion of the target-like residue. For the results presented here, nucleons contained in the projectile-like residue were not excluded.

The results are shown in Fig. 1. Consider first the calculations for the symmetric mass 40

system shown on the left hand side of the figure. Calculations for the soft equation of state and $4\pi\sigma_{nn}(\Omega)$=41 mb (parameter set 1 of table 1) are indicated by the solid circles. At low energies, attractive momentum transfers dominate; the majority of energetic nucleons are deflected by the attractive mean field and

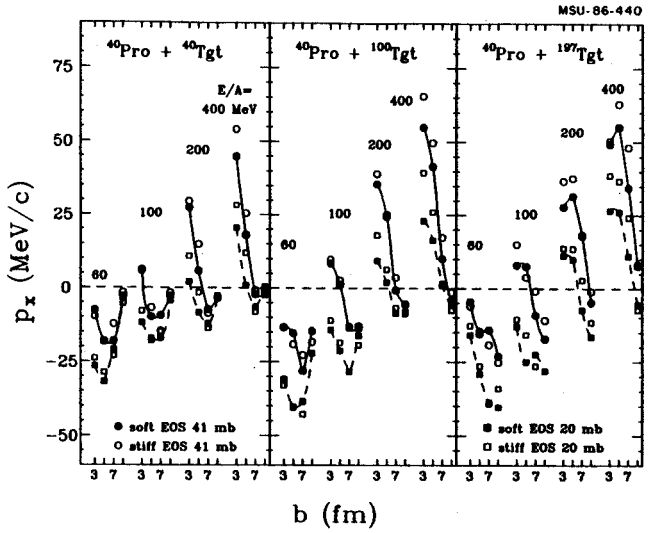

Fig.1. Mean transverse momenta calculated for mass 40 projectiles and mass 40, 100 and 197 targets, impact parameters of 3, 5, 7, and 9 fm, and bombarding energies of E/A = 60, 100, 200, and 400 MeV. The calculations are indicated by the solid circles and the solid lines for parameter set 1, the open circles for calculations with parameter set 2, the solid squares and dashed lines for parameter set 3 and the open squares for parameter set 4.

emerge with negative transverse momenta. The mean transverse momentum increases monotonically with bombarding energy. This is particularly evident at smaller impact parameters where $\langle P_x \rangle$ changes sign and goes rapidly positive for E/A > 100 MeV. A similar trend was reported in Ref. 2. These positive transverse momenta arise from the scattering of nucleons by the repulsive nuclear mean field present during the high density stage of the collision and from the kinetic pressure caused by the incoherent nucleon-nucleon collisions represented by the collision term.

The sensitivity to the equation of state is observed by comparing calculations with the same nucleon-nucleon cross section but different equations of state. The stiff equation of state (open points) provides slightly more positive values of $\langle P_x \rangle$ than the soft equation of state (closed points) at small impact parameters. $\langle P_x \rangle$ is more significantly altered by keeping the equation of state constant and changing the nucleon-nucleon cross section. The increase in $\langle P_x \rangle$ with increasing σ_{nn} is consistent with cascade calculations which showed an increase flow angle with increasing σ_{nn}.[3] Except for trivial geometrical effects in the impact parameter dependence, these trends are essentially preserved in the calculations with the heavier targets. Clearly, σ_{nn} must be accurately known before measurements of $\langle P_x \rangle$ can bongmha information concerning the equation of state.

References

1. J. Aichelin and G. Bertsch, Phys. Rev. C31 (1985) 1730 and references therein.
2. J.J. Molitoris, D. Hahn, and H. Stöcker, Nucl. Phys. A447 (1985) 13c.
3. M. Gyulassy, K.A. Frankel and H. Stöcker, Phys. Lett 110B (1982) 185.

TENSOR ALIGNMENT OF ^{7}Li AND ASTROPHYSICAL S-FACTOR FOR ^{4}He(t,γ)^{7}Li

T. Kajino, G.F. Bertsch, and K.-I. Kubo[a]

The tensor analyzing powers T_{20} for aligned ^{7}Li scattering from heavy nuclei are useful observables for studying the effect of E1 polarization of ^{7}Li. The present study[1] proposes a new method to determine the absolute strength of E1 astrophysical S-factor, the reaction rate, for the stellar nuclear process ^{4}He(t,γ)^{7}Li, which makes use of the theoretical relation between the E1 polarizability and the S-factor. This nuclear process and its mirror reaction ^{4}He(^{3}He,γ)^{7}Be followed by electron capture play an essential role to produce ^{7}Li in the big-bang expansion of the early universe.[2,3]

The new method consists of two procedures. First, we set up the polarization potential for aligned ^{7}Li scattering as

$$\langle i|V^{(2)}_{pol}|f\rangle = Y^*_{2\mu}(\hat{r}\cdot\hat{s})\, g \left\{\frac{4\pi}{5}\frac{Z_t e}{r^3}\langle i||M(E2)||f\rangle - \sqrt{\frac{9\pi}{5}}\frac{Z_t^2 e^2}{r^4}\tau_{if}\right\}, \quad (1)$$

$$\tau_{if} = \frac{8\pi}{9}\sqrt{\frac{10}{3}}\sum_n W(1\ 1\ I_i\ I_f\ ;\ 2\ I_n)\, \langle i||M(E1)||n\rangle\langle n||M(E1)||f\rangle/(E_n - E_i), \quad (2)$$

where M(Eλ) is the electric λ-pole operator, W(1 1 I_i I_f ; 2 I_n) is the Racah coefficient, g is the Clebsh-Gordan coefficient divided by $\sqrt{2I_i+1}$, and τ_{if} is the tensor moment of E1 polarizability. The first term in Eq. (1) represents the reorientation effect due to a large E2 moment of ^{7}Li, and the second term denotes the second order effect of virtual E1 excitation. There are four parameters in this potential; the E2 moment Q_s of the ground state, the B(E2) strength for the transition between the ground spin-doublets, and the E1 polarizabilities τ_{11} and τ_{12} of ^{7}Li. To constrain these, we have applied the following theoretical relations:

$$B(E2;\ 3/2^- \rightarrow 1/2^-) = \frac{25}{16\pi}(eQ_s)^2, \quad (3)$$

$$\tau_{11} = \tau_{12}. \quad (4)$$

These equations exactly hold true when we adopt the pure LS-coupling scheme for the wave function of ^{7}Li. It has been proved by many authors that the LS-scheme gives a very good approximation to the A=7 nuclear systems. We find also that the E1 polarizability τ_{if} is a negative quantity in this scheme. The average of the accumulated empirical data of the quadrupole moment was used to fix Q_s. Adopting these two constraints, we calculated T_{20} for ^{58}Ni(^{7}Li,^{7}Li) and ^{120}Sn(^{7}Li,^{7}Li) by using the program ECIS79. We have then determined the E1 polarizability τ_{if} by fitting the observed T_{20} data[4]; $\tau_{11} = -0.11$ fm^3.[1]

The second step is to determine the astrophysical S-factor with the use of extracted E1 polarizability. More than 95% of the radiative capture cross section for ^{4}He(t,γ)^{7}Li comes from the E1 transition among many possible multipole contributions in the low energy region E $\leq$ 25 MeV. In the LS-scheme, Eq. (2) is rewritten in terms of the astrophysical S-factor as

$$\tau_{if} = \sqrt{\frac{10}{3}}\frac{h\mu}{\pi^2}\sum_n e^{i\gamma}(-)^{I_n - I_f} W(1\ 1\ I_i\ I_f\ ;\ 2\ I_n) \int[S(E;\ I_n\rightarrow I_i)\, S(E;\ I_n\rightarrow I_f)]^{1/2} \exp(-2\pi\eta_c) (E+E_{th})^{-5/2}(E+|E_{th}-E_f|)^{-3/2}\, dE, \quad (5)$$

where $e^{i\gamma} = 1$ for τ_{11} and $(-)^{(2I_n+1)/2}$ for τ_{12}, and S(E; $I_n\rightarrow$I) is the astrophysical E1 S-factor.

Assuming only the energy dependence of the S-factor and the relative ratio of the s-wave ($I_n = 1/2^+$) to d-wave ($I_n = 3/2^+$ and $5/2^+$) contributions given by the microscopic cluster model calculation[5,6] for $^4He(t,\gamma)^7Li$, we extracted the S-factor from the determined τ_{if} values, as shown by solid curve in Fig. 1. The dashed curve corresponds to the previous analysis $|\tau_{if}| = 0.23$ fm^3 of Weller et al.[4] Note here that the sign of τ_{11} must be taken as negative to obtain a physical value for the S-factor, although Weller et al. could not determine the sign of τ_{if} in their analysis.

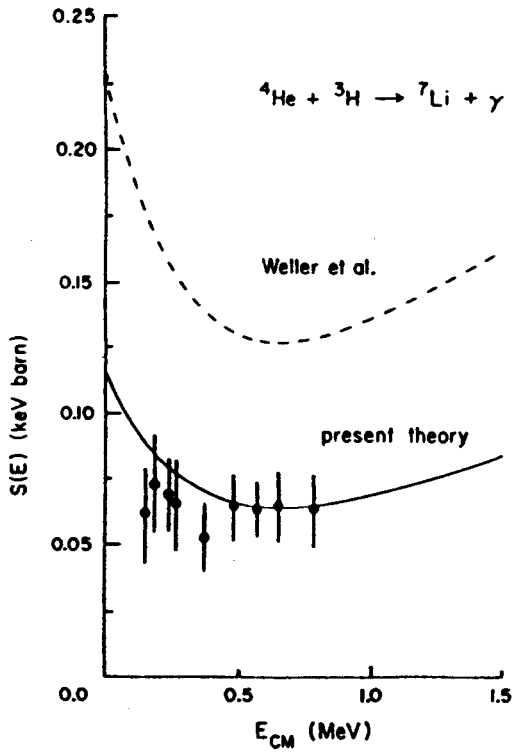

Fig. 1. Astrophysical S-factor for $^4He(t,\gamma)^7Li$. Experimental data are from Ref. 7. Solid and dashed curves correspond to the present (Ref. 1) and Weller's (Ref. 4) τ_{if} values, respectively.

For the $^4He(t,\gamma)^7Li$ reaction we obtain S(0) = 0.12 keV barn. This value should be compared with the observed ones 0.100 ± 0.025 keV barn[5,7] and 0.134 ± 0.03 keV barn[8] which were measured by using prompt γ-ray. With the scaling relation of the S(0)-factors between the two mirror reactions $^4He(t,\gamma)^7Li$ and $^4He(^3He,\gamma)^7Be$ found in the theoretical study[6], we obtain S(0) = 0.60 keV barn for the mirror $^4He(^3He,\gamma)^7Be$ reaction. This also is in a reasonable agreement with the weighted average 0.56 ± 0.03 keV barn[5] of the previous accepted data for this reaction.

The inferred τ_{if} values, and of course the S-factors too, are very sensitive to the adopted E2 moment of ^7Li. However, if the quoted accuracy of the atomic determination of Q_s can be trusted, then the nuclear measurements of the tensor analyzing powers for aligned ^7Li are just on the border of providing a useful determination of the astrophysical S-factors.

---

a. Tokyo Metropolitan University

References

1. T. Kajino, G.F. Bertsch, and K.-I. Kubo, submitted to Phys. Rev. C.
2. R.V. Wagoner, Astrophys. J. 178,343(1973).
3. S.M. Austin and C.H. King, Nature 269,782 (1977).
4. A. Weller et al., Phys. Rev. Lett. 55,480 (1985).
5. T. Kajino, H. Toki, and S.M. Austin, to be published in Astrophys. J. (1987).
6. T. Kajino, Nucl. Phys. A460,559(1986).
7. G.M. Griffiths et al., Can. J. Phys. 39 1397(1961).
8. U. Schroder et al., preprint of Munster University (1986).

APPLICATION OF TIME DEPENDENT DENSITY MATRIX METHOD TO $^{16}O+^{16}O$ REACTIONS

M. Tohyama

The time-dependent Hartree-Fock (TDHF) theory is a fully microscopic theory so far applied to heavy-ion collisions. Its application, however, is limited to low energy phenomena because of the neglect of nucleon-nucleon (NN) collision effects. Recently we have proposed the time dependent density matrix method (TDDM)[1] which incorporates NN collision effects into the mean field.

TDDM describes the time evolution of the one-body density matrix

$$\rho(r,r;t)=\sum_{\lambda\lambda'} n_{\lambda\lambda'}(t)\psi_\lambda(r,t)\psi^*_{\lambda'}(r',t)$$

where ψ_λ is single-particle (s.p.) wave function and $n_{\lambda\lambda'}$ is the occupation matrix. The equation of motion for ρ consists of two coupled equations. The first equation is a TDHF-like equation for s.p. wave functions

$$i\frac{\partial}{\partial t}\psi_\lambda(r,t)=[-\frac{\nabla^2}{2m}+U_{HF}(\rho)]\psi_\lambda(r,t)$$

$$=h\psi_\lambda(r,t)$$

where $U_{HF}(\rho)$ is the mean potential including NN collision effects through ρ. The second equation is for the occupation matrix

$$\frac{d}{dt}n_{\lambda\lambda'}(t)=-[F_{\lambda\lambda'}(t)+F^*_{\lambda'\lambda}(t)]$$

where $F_{\lambda\lambda'}$ is defined as

$$F_{\lambda\lambda'}(t)=\sum_{\alpha\alpha'\beta\beta'\gamma\delta\delta'}\langle\lambda\delta'|v|\alpha\beta\rangle|_t$$

$$\times\int_{-\infty}^{t}dt'\langle\alpha'\beta'|v|\gamma\delta\rangle|_{t'}$$

$$\times\{[\delta_{\alpha\alpha'}-n_{\alpha\alpha'}(t')][\delta_{\beta\beta'}-n_{\beta\beta'}(t')]n_{\gamma\lambda'}(t')n_{\delta\delta'}(t')$$

$$-[\delta_{\gamma\lambda'}-n_{\gamma\lambda'}(t')][\delta_{\delta\delta'}-n_{\delta\delta'}(t')]n_{\alpha\alpha'}(t')n_{\beta\beta'}(t')\{$$

Here v is the residual interaction. The equation of motion for ρ conserves the total number of particles, the total momentum, and the total energy consisting of the HF energy and the correlation energy.[1]

We applied TDDM to head-on collision of $^{16}O+^{16}O$ at low energies to investigate the fusion window anomaly predicted by TDHF calculations.[2] We used TDHF code with axial symmetry[3] and the effective interaction of Ref. 4. The residual interaction was assumed to be $v(r-r')=v_0\delta^3(r-r')$ with $v_0=-300MeVfm^3$. S.p. states were taken up to the 2s-1d shell. The 1s and 1p orbits are initially completely occupied.

The time evolution of the diagonal elements of $n_{\lambda\lambda'}$ is shown in the upper part of Fig. 1. The incident energy is $E_{lab}=100MeV$. The lower part of Fig. 1 shows the time evolution of the diagonal s.p. energies defined by $\varepsilon_{\lambda\lambda}=\langle\lambda|h|\lambda\rangle$. Although there is no crossing in the s.p. energies between the occupied and unoccupied states, NN collisions occur. This is due to the t' integration in $F_{\lambda\lambda'}$. (Memory effects.) Fig. 2 shows the time evolution of the relative distance between two fragments at $E_{lab}=100MeV$. At this energy there is no fusion in TDHF. The system fuses in TDDM as can be seen in Fig. 2. Since the final kinetic energy of the relative motion in TDHF is very close to the Coulomb barrier, a small additional damping of the relative motion leads the system to fusion. We found that the threshold energy is increased from $E_{lab}=54$ MeV (TDHF) to $E_{lab}=140$ MeV.

References

1. M. Tohyama, Phys. Lett. 163B,14(1985); preprint MSUCL-591, January 1987.
2. J. W. Negele, Rev. Mod. Phys. 54,913(1982).
3. K. T. R. Davies and S. E. Koonin, Phys. Rev. C. 23,2042(1981).
4. P. Bonche, S. E. Koonin, and J .W. Negele, Phys. Rev. C 13,1226(1976).
5. M. Tohyama, Phys. Lett. 160B,235(1985).

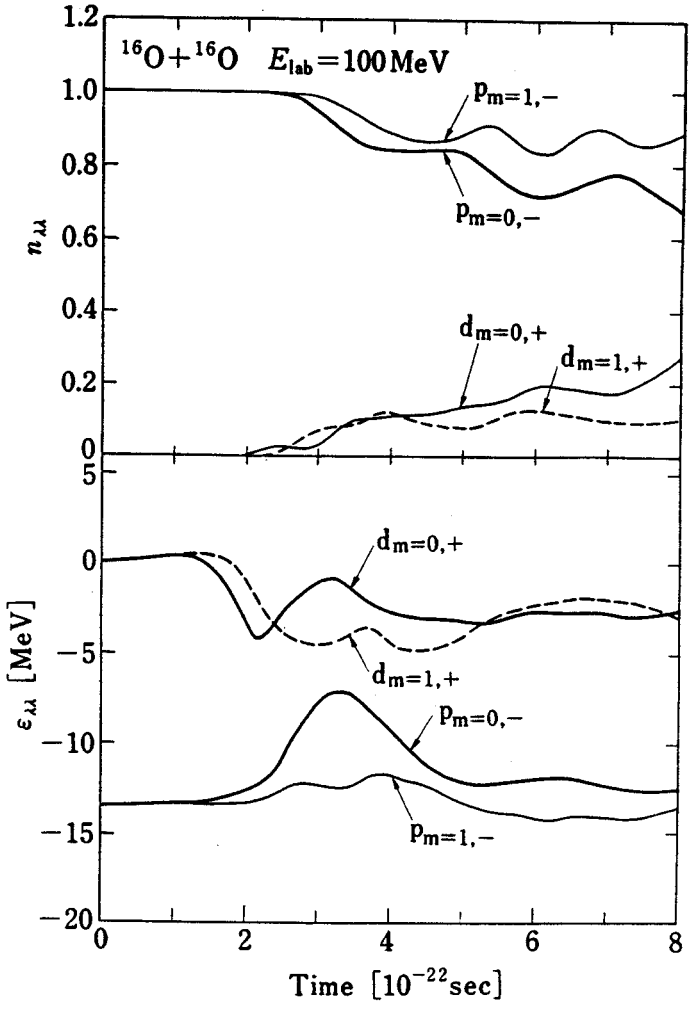

Fig. 1 Time evolution of the diagonal elements of the occupation matrix (upper part) and that of the s.p. energies (lower part) at E_{lab}=100 MeV. The s.p. states are labeled by the asymptotic quantum numbers.

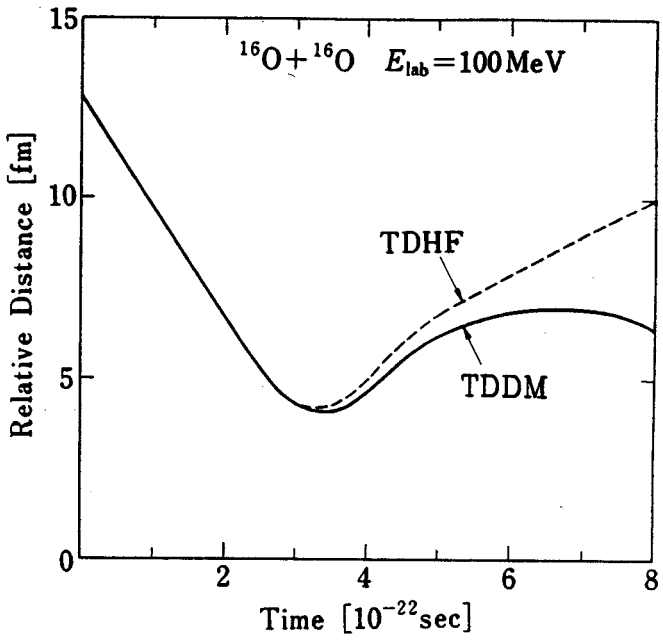

Fig. 2 Time evolution of the relative distance between two fragments at E_{lab}=100 MeV. The solid curve denotes the TDDM result and the dashed curve the TDHF one.

QUANTUM EFFECTS ON HIGH ENERGY γ PRODUCTION IN HEAVY ION COLLISIONS

M. Tohyama

The production mechanism of high-energy γ's from intermediate energy heavy-ion collisions has been studied with various theoretical models and there seems to be a consensus that the dominant elementary process is p+n→p+n+γ. Recently Bauer et al.[1] made an analysis of proton neutron collision effects on γ production, based on the BUU model. Although it can reproduce essential features of experimental data, there seems to be some problems with the incident energy dependence of γ production rate; the BUU calculation gives a little weaker incident energy dependence than experiment. This may be attributed to the quantum effects e.g. shell effects which are not included in the semiclassical approach like the BUU. The aim of this work is to analyze such effects for simple one-dimensional systems.

We use the TDHF model which has been applied to pion and γ production.[2] The results in the TDHF model are compared with those in its semiclassical limit. Since our interests are in the available nucleon phase space, we use a simple interaction for the elementary production process i.e. N+N→N+N+γ

$$e^{ikz}\delta(z-z')$$

where the photon wave function is approximated by the plane wave and the photon polarization is neglected. In the TDHF model the number distribution of photons with momentum k is given for this interaction by

$$\omega\frac{dN}{dk}\propto\sum_{\rho\rho'\nu\nu'}\left|\int_{-\infty}^{\infty}dzdte^{i\omega t-ikz}\right.$$
$$\left.\times\psi^*_\rho(zt)\psi^*_{\rho'}(zt)\psi_\nu(zt)\psi_{\nu'}(zt)\right|^2 \qquad (1)$$

where $\{\psi_\rho\}$ are s.p. wave functions for unoccupied states and $\{\psi_\nu\}$ for occupied states. The s.p. wave functions obey the TDHF equation.

Equation (1) can be expressed in terms of the distribution functions defined as

$$\rho(xt,x't')=\sum_\nu\psi_\nu(xt)\psi^*_\nu(x't')$$

$$\tilde\rho(xt,x't')=\sum_\rho\psi_\rho(xt)\psi^*_\rho(x't')$$

The Fourier transforms of ρ and $\tilde\rho$

$$\rho(zt,z't')=\int\frac{dkd\omega}{2\pi2\pi}f(k,\omega,Z,T)e^{ik\zeta-i\omega\tau}$$

$$\tilde\rho(zt,z't')=\int\frac{dkd\omega}{2\pi2\pi}\tilde f(k,\omega,Z,T)e^{ik\zeta-i\omega\tau}$$

where $\zeta=z-z'$, $Z=(z+z')/2$, $\tau=t-t'$, and $T=(t+t')/2$ can be also used to express dN/dk. In the classical limit the energy-momentum relation is approximated by

$$f(k,\omega,Z,T)=2\pi\delta(\omega-\frac{k^2}{2m}-U(Z,T))f(k,Z,T)$$

$$\tilde f(k,\omega,Z,T)=2\pi\delta(\omega-\frac{k^2}{2m}-U(Z,T))[1-f(k,Z,T)] \qquad (2)$$

where U(Z,T) and f(k,Z,T) are the mean potential and the momentum distribution at Z and T, respectively. The number distribution in the semiclassical limit becomes

$$\omega\frac{dN}{dk}\propto(2\pi)^{-4}\int_{-\infty}^{\infty}dZdTdk_1dk_2dk_3dk_4$$
$$\times2\pi\delta(\omega+\varepsilon_1+\varepsilon_2-\varepsilon_3-\varepsilon_4)2\pi\delta(k+k_1+k_2-k_3-k_4)$$
$$\times\bar f(k_1,Z,T)\bar f(k_2,Z,T)f(k_3,Z,T)f(k_4,Z,T) \qquad (3)$$

where the energy is given by $\varepsilon=k^2/2m$.

The numerical calculation is performed for one-dimensional fragments each consisting of eight nucleons. There is an energy gap of about 15 MeV between occupied and unoccupied s.p. states. The HF potential is the same as that used by Richert et al.[3] which was deduced from the Skyrme interaction. The momentum distribution f(k,Z,T) used in Eq. (3) is

calculated with the TDHF s.p. wave functions. The number distribution of produced photons is shown in Fig. 1. The closed squares and dots denote the results in the TDHF model at $E_{lab}/A=$ 20 and 40 MeV, respectively. The open squares and circles indicate the results in the semiclassical model at $E_{lab}/A=$ 20 and 40 MeV, respectively. The TDHF results differ from the semiclassical ones in three aspects: (1) The TDHF model predicts smaller production rates than the semiclassical model. (2) The incident energy dependence of production rates in the TDHF model is larger than that in the semiclassical model. (3) The slope in the TDHF model is less steep in the low energy region of photon. The first two points can be attributed to an energy gap between occupied and unoccupied states. The energy gap becomes less important as the beam energy increases. This explains a larger incident energy dependence in the TDHF model. The last point that the TDHF model gives a less steep slope in the low photon energy region is due to the structural difference between initial and final wave functions. These effects are washed out in the semiclassical approximation Eq. (2).

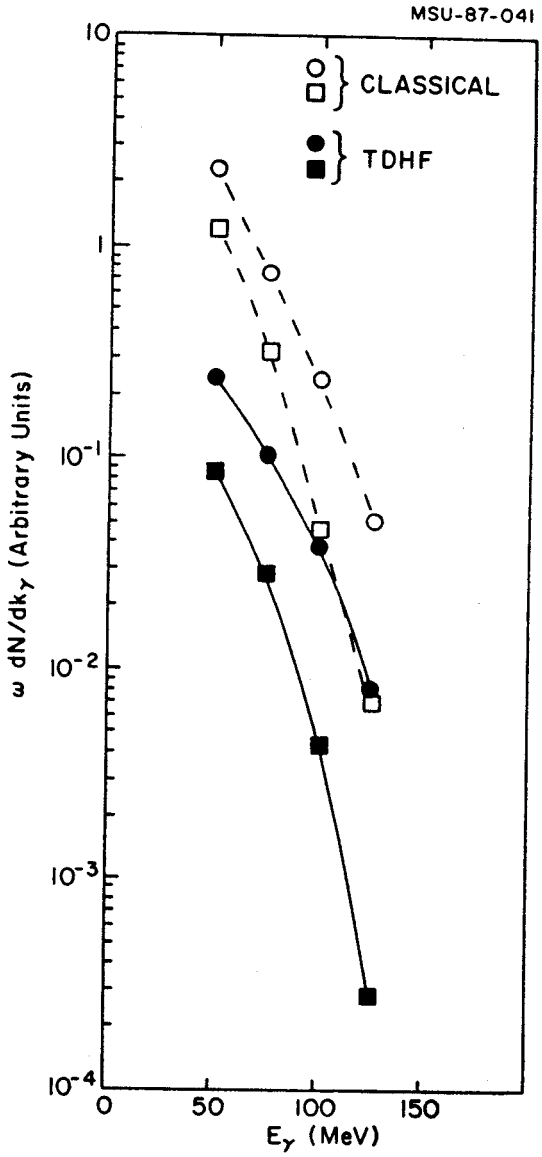

Fig. 1. Incident energy dependence of γ spectrum. The open circles and squares denote the semiclassical results at $E_{lab}/A=40$ and 20 MeV, respectively and the closed circles and squares the TDHF results at $E_{lab}/A=40$ and 20 MeV, respectively.

References

1. W. Bauer, G.F. Bertsch, W. Cassing, and U. Mosel, Phys. Rev. C. 34,2127(1986)
2. M. Tohyama, R. Kaps, D. Masak, and U. Mosel, Nucl. Phys. A437,739(1985); W. Bauer, W. Cassing, U. Mosel, M. Tohyama, R.Y. Cusson, Nucl. Phys. A456,159(1986)
3. J. Richert, D.M. Brink, and H.A. Weidenmüller, Phys. Lett. 87B,6(1979)

LIGHT PARTICLE CORRELATIONS IN HEAVY ION COLLISIONS

W. Bauer[a]

Commonly the BUU equation is solved in the test particle simulation[1] with n test particles per nucleon. Here we propose a modification of the equations of motion for the test particles which enables us to explicitly assure total momentum conservation[2]. Instead of propagating $n(A_T + A_p)$ test particles, we simultaneously propagate n events of $A_T + A_p$ nucleons each. The nucleon-nucleon collisions in the cascade part $C(\vec{p})$ are restricted to collisions between nucleons in the same event. It is now possible to enforce conservation of momentum in every event separately at every time instant via

$$\frac{d\vec{r}_j}{dt} = \vec{p}_j/m_j$$

$$\frac{d\vec{p}_j}{dt} = -\vec{\nabla}U(\rho(\vec{r}_j)) + \vec{q} + C(\vec{p}_j)$$

$$\vec{q} = \frac{\sum_{k=1}^{A_T+A_p} \vec{\nabla}U(\rho(\vec{r}_k))}{A_T + A_p}$$

$$j = 1,\ldots,(A_T + A_p)$$

The phase space density $f(\vec{r},\vec{p},t)$ is averaged over all n events to assure the same accuracy in the evaluation of the mean field potential $U(\rho)$ and the Pauli-blocking factors $1 - f(\vec{r},\vec{p},t)$ as in the conventional BUU approach.

With this modification it is possible to study the effect of the momentum conservation law on proton-proton coincidence spectra. Except for the correlations due to this conservation law and the correlations due to nucleon-nucleon collisions no other correlations are included in this framework.

We define the two-particle correlation function

$$C(\theta_1,\theta_2,\phi,\Delta E_1,\Delta E_2) = \frac{\sigma_R \cdot \sigma_{12}}{\sigma_1 \cdot \sigma_2}$$

$$= \frac{\sigma_R \cdot \int_{\Delta E_1} dE_1 \int_{\Delta E_2} dE_2 \frac{d^4\sigma_{12}(E_1,E_2,\theta_1,\theta_2,\phi)}{dE_1\, d\Omega_1\, dE_2\, d\Omega_2}}{\int_{\Delta E_1} dE_1 \frac{d^2\sigma_1(E_1,\theta_1)}{dE_1\, d\Omega_1} \cdot \int_{\Delta E_2} dE_2 \frac{d^2\sigma_2(E_2,\theta_2)}{dE_2\, d\Omega_2}}$$

where θ_1 and θ_w are the emission angles of the two particles with respect to the beam axis and ϕ is their relative azimuthal angle. ΔE_1 and ΔE_2 are the detector energy intervals for the two particles. σ_R is the reaction cross section. In case of statistically indepedent emission the correlation function always has the value $C(\theta_1,\theta_2,\phi,\Delta E_1,\Delta E_2) = 1$. Values of $C < 1$ mean a supression and $C > 1$ an enhancement of the emission of particle 2 due to the coincident emission of particle 1.

For the reaction 25 MeV/nucleon $^{16}O + ^{12}C \rightarrow 2p + X$ we have compared our results (histograms) to the experimental data (circles)[3]. The angle θ_1 was 40°. The most obvious feature from Fig. 1. is the fact that the two-proton correlation function is always smaller than 1 which means that the coincident emission of particle 2 with particle 1 is supressed. This reflects a microcanonical effect due to the finiteness of the available energy and particle number. The data also show an increasing value of the correlation function with increasing relative angle ϕ. This effect is due to the conservation of overall momentum and also reproduced by the calculations. Due to the emission of the trigger particle the remaining system experiences a "recoil" resulting in the

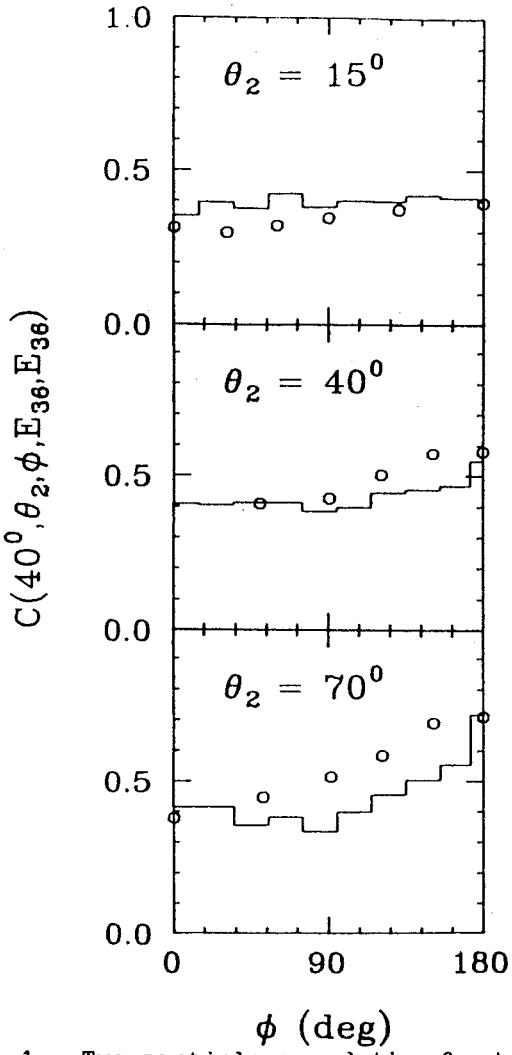

Fig. 1. Two-particle correlation function for the reaction $^{16}O + ^{12}C \rightarrow 2p + X$ at 25 MeV/nucleon. Experimental data is shown as circles, compared with theory histogram.

preferred emission of the second particle under $\phi = 180°$.

In fig. 2 the in-plane/out-of-plane ratio $R(\theta_1,\theta_2,\Delta E_1,\Delta E_2) := \frac{C(\theta_1,\theta_2,180°\Delta E_1,\Delta E_2)}{C(\theta_1,\theta_2,90°\Delta E_1,\Delta E_2)}$ is plotted. The data[4] are represented by circles and our calculations by histograms. The system under consideration is 40 MeV/nucleon $^{12}C + ^{12}C \rightarrow 2p + X$. The trigger detector was placed at $\theta_1 = 45°$. Generally the ratio R is larger than 1, again reflecting the effects of momentum conservation. There is no particular enhancement of R visible at $\theta_2 = 45°$ which would correspond to a quasielastic p-p scattering. The reason for this is to be found in the wide distribution of nucleon-nucleon center-of-mass momenta for individual collisions due to the Fermi motion of the nucleons.

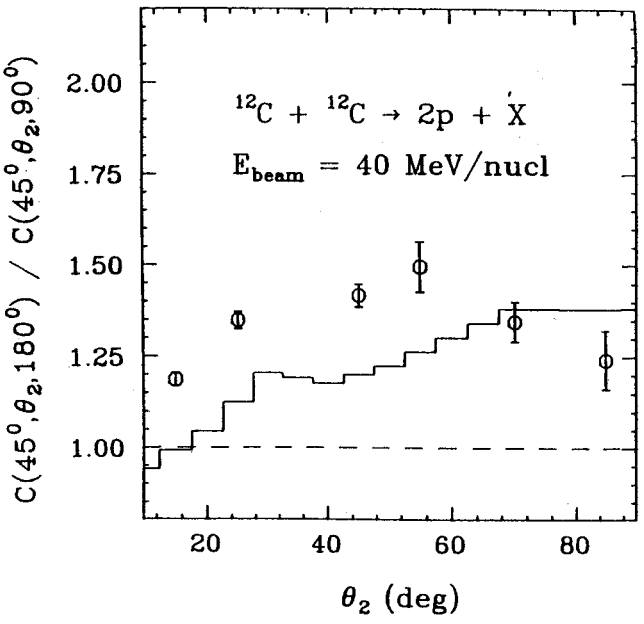

Fig. 2. In-plane/out-of-plane ratio for the reaction $^{12}C+^{12}C \rightarrow 2p + X$ at 40 MeV/nucleon. Data from ref. [4] is compared with theory histogram.

---

a. Supported by Studienstiftung des deutschen Volkes

References

1. G.F. Bertsch et al., Phys. Rev. C29, 673 (1984).
2. W. Bauer, submitted to Nucl. Phys. A.
3. C.B. Chitwood et al., Phys. Rev. C34, 858 (1986).
4. D. Fox and G.D. Westfall, private communication.